The Depth Variability of Meridional Gradients of Temperature, Salinity and Sound Velocity in the Western North Pacific[1]

GUNNAR I. RODEN

Department of Oceanography, University of Washington, Seattle 98195

(Manuscript received 21 August 1978, in final form 12 January 1979)

ABSTRACT

In the western North Pacific, meridional gradients of temperature, salinity and sound velocity show considerable variation with depth. Gradients of frontal intensity (more than three times the rms value) occur in the upper 600 m of the ocean. Fronts in the surface layer are spaced at irregular intervals. Many deep fronts have no surface manifestation and are spaced at intervals between 300 and 600 km. A spectral analysis of the meridional gradients as functions of depth and longitude was carried out for the wavenumber range between 0 and 13.4 cycles per 1000 km (c.p. 1000 km). The shape of the power density spectra strongly depends on depth. In the upper 150 m the shape is irregular. Between 300 and 600 m, the spectra show a well-defined peak between 1.5 and 3.3 c.p. 1000 km and a sharp decrease in power beyond 10 c.p. 1000 km. While the shape of the power density spectra shows little variation with longitude, there is a substantial decrease in the total power when crossing the Emperor seamount chain. Meridional gradients at the sea surface are coherent with those in the upper 150 m and incoherent with those below. Meridional gradients at 300 m have a good coherence with those at greater depths. The coherence between meridional temperature and salinity gradients increases with increasing depth. The depth dependence of the spectra and coherence is attributed to different processes of gradient formation in the upper and lower layers of the sea. A comparison of the wavenumber spectra of the meridional gradients with the wavenumber spectra of zonal gradients derived from Bernstein and White's (1977) and Wilson and Dugan's (1978) data shows that in each case the dominant spectral peak occurs between about 1.5 and 3 c.p. 1000 km, indicating the prevalence of features with zonal and meridional wavelengths in the 300–600 km range.

1. Introduction

The western Pacific is noted for numerous fronts (Uda, 1938; Roden, 1975), eddies (Bernstein and White, 1974, 1977) and Rossby-type long waves (Kawai, 1972; Cheney 1977; Roden, 1977), which occur together and give rise to a complicated thermohaline structure. In March and April 1971, the R.V. *Thomas G. Thompson* made three long meridional sections in the area (Fig. 1). The extraordinary complexity of the thermohaline structure is revealed in Fig. 2, which shows a sound velocity section along longitude 168°E, between latitudes 43° and 20°40'N. The 2500 km long section is based on 37 km horizontal and 3 m vertical sampling intervals. Frontal features, associated with strong meridional gradients, appear in black (for the purpose of this paper, meridional gradients exceeding three times the rms value over the section will be regarded as fronts). Fronts are found to occur not only in the upper wind stirred layer, but also at greater depths. Many of the deep fronts have no surface manifestation. In the upper 150 m, fronts are spaced at irregular intervals, while those below have a tendency to occur at regular intervals apart. This difference between surface and deep fronts points to different dynamic processes of formation. In the upper layer, fronts separate water masses of different origin and form primarily in response to differential *horizontal* advective and surface exchange processes, which vary considerably from one geographical region to another. In the deep layer, where vertical stratification is dominant, fronts form primarily in response to differential *vertical* advective processes. When the vertical velocity is influenced by wave motion, regularly spaced fronts can be expected. Similar conditions are known to exist in the atmosphere, where the dynamics of lower and upper tropospheric fronts are fundamentally different (Palmén and Newton, 1969; Shapiro, 1970).

In order to describe the complicated structure shown in Fig. 2, it is convenient to regard the meridional gradients as stochastic variables and analyze them by spectral analysis methods. The

[1] Contribution No. 1065 from the Department of Oceanography, University of Washington.

0022-3670/79/040756-12$07.00

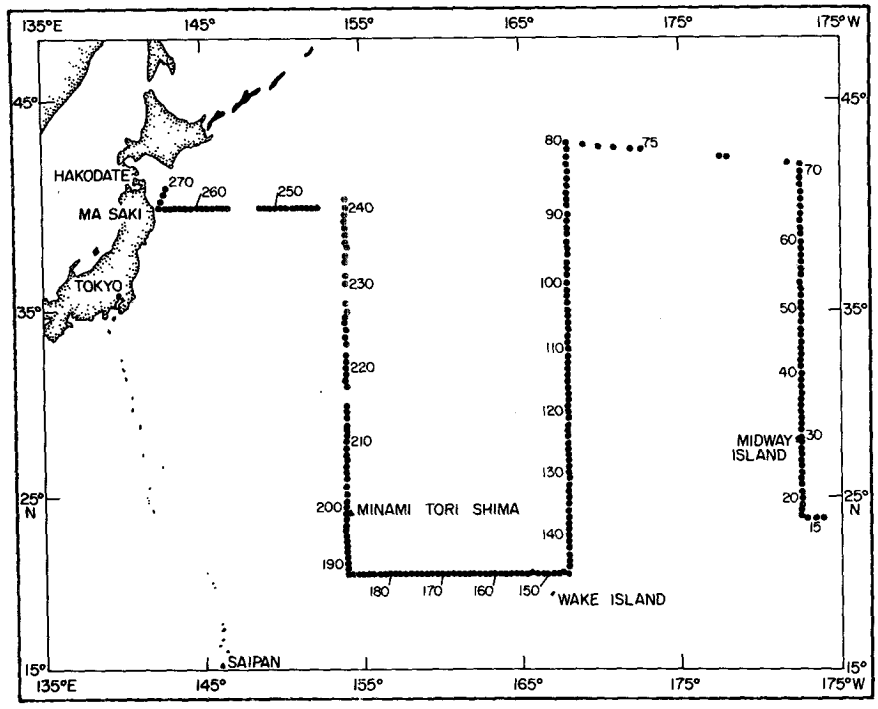

FIG. 1. Stations occupied during the 58th voyage of the R.V. *Thomas G., Thompson*, 19 March–3 May 1971.

following questions become relevant then: 1) What are the typical rms and extreme values of the meridional gradients at different depths? 2) How does the spectral density of the meridional gradients change with meridional wavenumber and are there any preferred wavenumbers at which the spectral density is concentrated? 3) How do the spectral densities change with depth and longitude? 4) For a given variable, what is the depth coherence of its meridional gradients? 5) For a given depth, how are the meridional gradients of different variables, such as temperature and salinity, related?

2. Data

The following analysis is based on STD data collected during the 58th cruise of the R.V. *Thomas G. Thompson* in March and April 1971 (Roden, 1972). Temperatures and salinities were measured directly, to an accuracy of 0.01°C and 0.03‰, respectively. Sound velocity was computed from Wilson's equation (Tolstoy and Clay, 1966) using STD temperatures and salinities as input. The thermohaline gradients were computed by the central difference approximation for six depths: 0, 150, 300, 450 and 600 m. The Tukey method was used to compute the wavenumber spectra. The computations were carried out for the wavenumber range between 0 and 13.4 cycles per 1000 km (c.p. 1000 km), with a resolution of 0.6 c.p. 1000 km. This allows one to detect dominant wavelengths from 75 to about 800 km.

Zonal wavenumber spectra published by Bernstein and White (1977) and Wilson and Dugan (1978) were utilized for comparison. The conversion from the original temperature spectra to temperature gradient spectra was achieved by multiplying the original spectra by the zonal wave-number squared.

3. Observed meridional gradients and their rms and extreme values

The observed meridional gradients of temperature, salinity and sound velocity along longitude 168°E are shown in Fig. 3. The outstanding feature is the change of the character of the gradients with depth. At the sea surface, the meridional gradient associated with the subarctic front (near 42°N) dominates over all others and the spacing between the peaks is irregular. At 300 m and below, the amplitudes of the positive and negative gradients are more equal and the peaks are spaced at rather regular intervals, which suggests wave motion. The distance between crests varies between 400 and 500 km, which indicates that Rossby-type waves could be involved (Longuet-Higgins, 1965; Philander, 1978). At present, the above argument must be regarded as tentative, because it is impossible to prove the exact origin of the quasi-

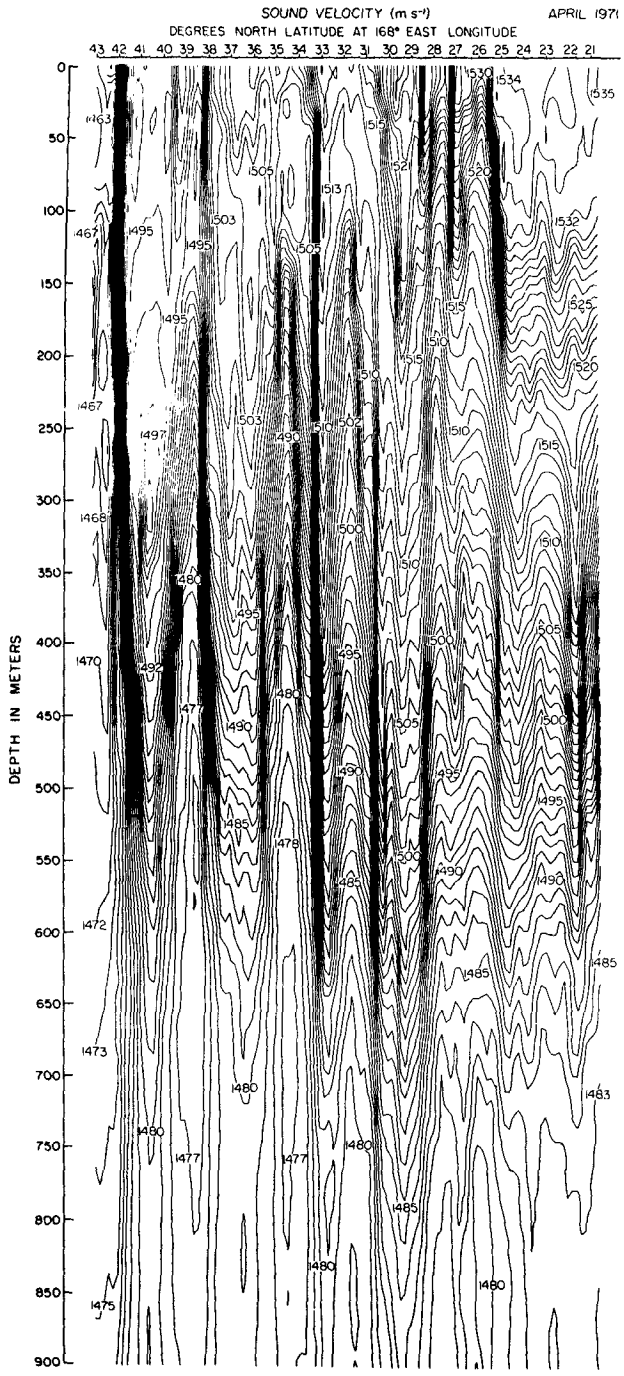

FIG. 2. Meridional sound velocity section along longitude 168°E, obtained between 3 and 11 April 1971. The contour interval is 1 m s^{-1}. Frontal features associated with strong meridional gradients appear in black.

regularly spaced oscillations from the limited data at hand.

The rms and extreme amplitudes of the meridional gradients are listed in Table 1 as functions of longitude and depth. It is seen that the strongest meridional gradients occur frequently at subsurface depths rather than at the sea surface and that the rms and extreme amplitudes are substantially larger at longitudes 154°E and 168°E than at longitude 177°20′W. The major topographic feature in the region is the Emperor seamount chain near 170°E, which rises up to 4500 m from the surrounding sea floor and comes to within 800 m of the sea surface in places. West of the Emperor seamount chain, rms amplitudes of the meridional gradients reach 2.2°C (100 km)$^{-1}$ for temperature, 0.3‰ (100 km)$^{-1}$ for salinity and 7.9 m s^{-1} (100 km)$^{-1}$ for sound velocity. East of this chain, the corresponding values for 1.3°C (100 km)$^{-1}$, 0.1‰ (100 km)$^{-1}$ and 4.2 m s^{-1} (100 km)$^{-1}$, respectively. Extreme amplitudes of the meridional gradients west of the chain are 8.2°C (100 km)$^{-1}$ for temperature, 1.4‰ (100 km)$^{-1}$ for salinity and 29.7 m s^{-1} (100 km)$^{-1}$ for sound velocity. East of the chain, the extreme amplitudes are about half of the above mentioned. The large eastward decrease of the amplitude of the temperature perturbations across the Emperor seamount chain was noted also by Bernstein and White (1977).

4. Spectra of meridional gradients

The power density spectra for the meridional gradients of temperature, salinity and sound velocity at 168°E are shown in Fig. 4 for the meridional wavenumber range from 0.6 to 13.4 c.p. 1000 km. The arrows indicate the 80% confidence limits. The shape of the power density spectra depends strongly upon depth. In the upper 150 m, where meridional gradients are formed mainly by differential horizontal advective and surface exchange processes, the spectra are irregular in shape and do not show any significant peaks. Between 300 and 600 m, where meridional gradients are largely formed by differential vertical advective processes, the spectra show a well-defined peak at a wavenumber of 2.43 c.p. 1000 km, which corresponds to a dominant wavelength of 411 km. The meridional wavenumbers corresponding to the half peak-power densities are 1.5 and 3.3 c.p. 1000 km, approximately, indicating that wavelengths between 300 and 666 km are fairly common also. Beyond meridional wavenumbers of 10 c.p. 1000 km, the power density becomes very low, which suggests a cutoff for waves of length of less than about 100 km. The peak power density decreases with depth rapidly between 300 and 600 m. For meridional gradients of temperature and sound velocity, the decrease is 25% between 300 and 450 m and 70% between 300 and 600 m. For meridional gradients of salinity, the corresponding values are 53 and 83%, respectively. The different attenuation rates for temperature and salinity are not fully understood at present.

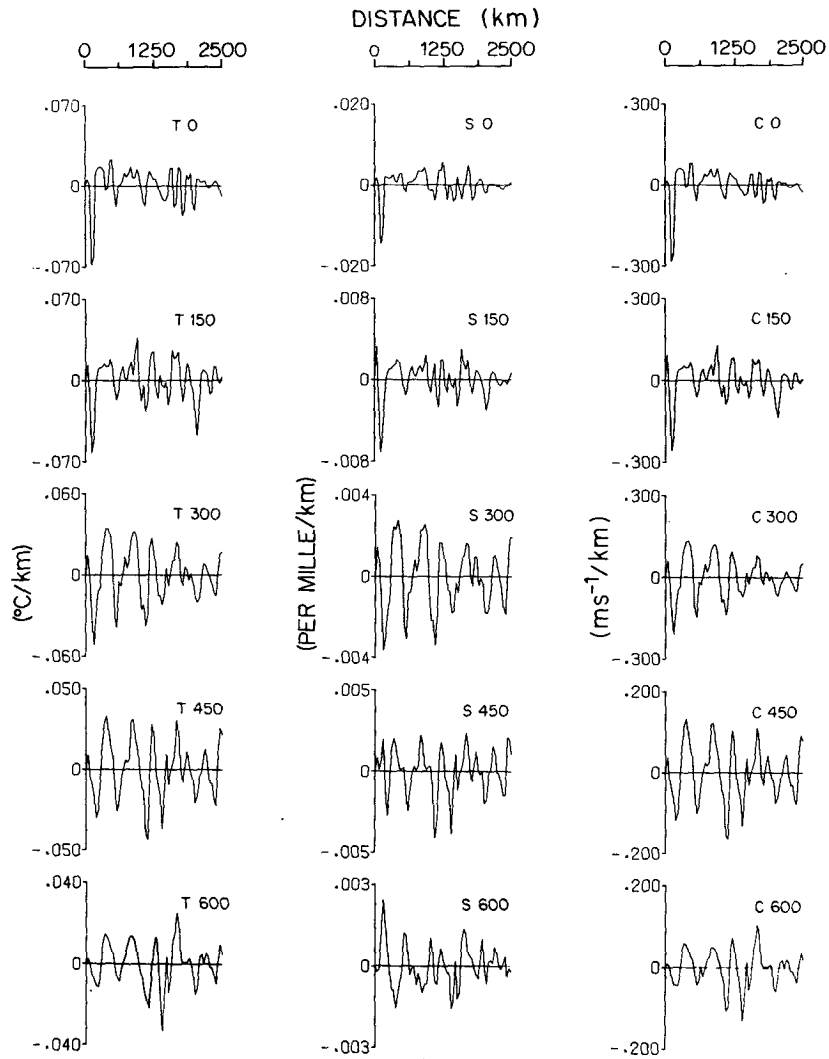

FIG. 3. Meridional gradients of temperature, salinity and sound velocity along longitude 168°E obtained in early April 1971. North is to the left.

5. Longitudinal variation of the spectra of meridional gradients

The above description has dealt exclusively with meridional wave-number spectra at longitude 168°E. It is of interest to know how representative these results are at other longitudes and, in particular, whether differences occur in the spectra west and east of the Emperor seamount chain. In Fig. 5 are shown the spectra of meridional gradients of temperature, salinity, sound velocity and density as a function of longitude. The arrows indicate the 80% confidence limits.

At all longitudes, the spectra show a broad peak in the wavenumber range between about 1.5 and 4.5 c.p. 1000 km and a sharp decrease in spectral density beyond 10 c.p. 1000 km, indicating a prevalence of waves with lengths between 222 and 666 km and a scarcity of those with lengths of less than 100 km. There is a sharp drop of the spectral density levels between 168°E and 177°20'W, with the levels west of the Emperor seamount chain (near 170°E) exceeding those to the east of the chain by a factor of 2–4.

A closer examination of the spectra shows that the highest peaks occur at a wavenumber of 3.64 c.p. 1000 km at longitude 154°E, at 2.43 c.p. 1000 km at longitude 168°E and at 3.04 c.p. 1000 km at longitude 177°20'W. The corresponding wavelengths are 274, 411 and 329 km, respectively. It is not possible to assess the significance of these differences in wavelengths, because of the shortness of the available records. If real, the differences would indicate a decrease in wavelength away from 168°E, the longitude closest to the Emperor seamount chain.

TABLE 1. rms and extreme amplitudes of meridional temperature gradients [°C(100 km)$^{-1}$] meridional salinity gradients [‰(100 km)$^{-1}$] and meridional sound velocity gradients [m s^{-1}(100 km)$^{-1}$] in the western Pacific.

Variable	Depth (m)	Longitude					
		154°00'E		168°00'E		177°20'W	
		rms	extreme	rms	extreme	rms	extreme
Temperature gradient	0	1.52	5.3	1.51	6.8	0.97	2.6
	150	1.93	8.2	1.83	6.3	1.33	4.9
	300	2.16	6.9	1.95	5.2	0.92	2.4
	450	1.82	5.4	1.76	4.3	0.83	2.4
	600	1.14	2.9	1.05	3.3	0.60	1.2
Salinity gradient	0	0.13	0.4	0.31	1.4	0.13	0.3
	150	0.15	0.7	0.17	0.7	0.13	0.4
	300	0.18	0.6	0.16	0.4	0.10	0.2
	450	0.14	0.5	0.14	0.4	0.08	0.3
	600	0.10	0.3	0.08	0.2	0.04	0.1
Sound velocity gradient	0	4.58	18.0	5.91	28.4	3.09	7.3
	150	6.59	29.7	6.46	25.8	4.24	14.4
	300	7.95	24.7	7.30	20.9	3.33	7.9
	450	6.95	20.6	6.80	16.5	3.21	9.1
	600	4.50	11.4	4.17	13.1	2.43	5.0

6. Depth coherence of meridional gradients

An important problem in the analysis of oceanic fronts is the depth coherence of horizontal gradients of temperature, salinity and sound velocity. The coherence between the meridional gradients at the sea surface and those at subsurface depths is shown in Fig. 6 for the wavenumber range between 0 and 13.4 c.p. 1000 km. The dashed line indicates the 95% confidence limit. The meridional gradients at 0 and 150 m are coherent over the entire wavenumber range, indicating that frontogenetic processes in the upper mixed layer are similar. As the depth increases, the coherence with the surface signature drops. At 300 m and below, significant coherence is found only in a narrow wavenumber range centered around 2.43 c.p. 1000 km. Even there, no more than 40 to 60% of the variance of the meridional gradients is related to the variance at the sea surface. This suggests that frontogenetic processes in the layer above and below the pycnocline are different.

The above is relevant for remote sensing from space. Satellite imagery of the sea surface temperature gradients and salinity gradients can be used only to detect upper layer temperature and salinity fronts. The horizontal thermohaline structure below pycnocline depth cannot be inferred from infrared and colorimetric measurements from space.

In contrast to the poor coherence between surface and deep meridional gradients, the gradients below pycnocline depth are strongly related to each other. This is shown in Fig. 7, where the meridional sound velocity gradients at 300 m are related to those at other depths. In the depth range between 150 and 600 m there is statistically significant coherence at all wavenumbers between 0 and 13.4 c.p. 1000 km. The phase (not shown) does not vary by more than 10° from zero, indicating that the fluctuations are in phase over the depth range investigated.

7. Coherence between meridional gradients of temperature and salinity

The coherence between meridional gradients of temperature and salinity is shown in Fig. 8 for different depths. There is statistically significant coherence at all depths and over the entire wavenumber range. The coherence is better at subsurface depths than at the sea surface. This is not surprising, because temperatures and salinity at the sea surface are influenced by the largely independent processes of radiative heat transfer and rainfall, which affect one variable but not the other. At greater depths, where the influence of surface processes is not felt, temperature and salinity can be regarded as passive variables, carried along by particle motion. Here a close correspondence can be expected among temperature, salinity and velocity gradients (Kirwan, 1975).

8. Notes on zonal thermohaline gradients in the western Pacific

The discussion so far has dealt with meridional thermohaline and sound velocity gradients in the western Pacific and the question arises as to the character of the zonal gradients. Unfortunately,

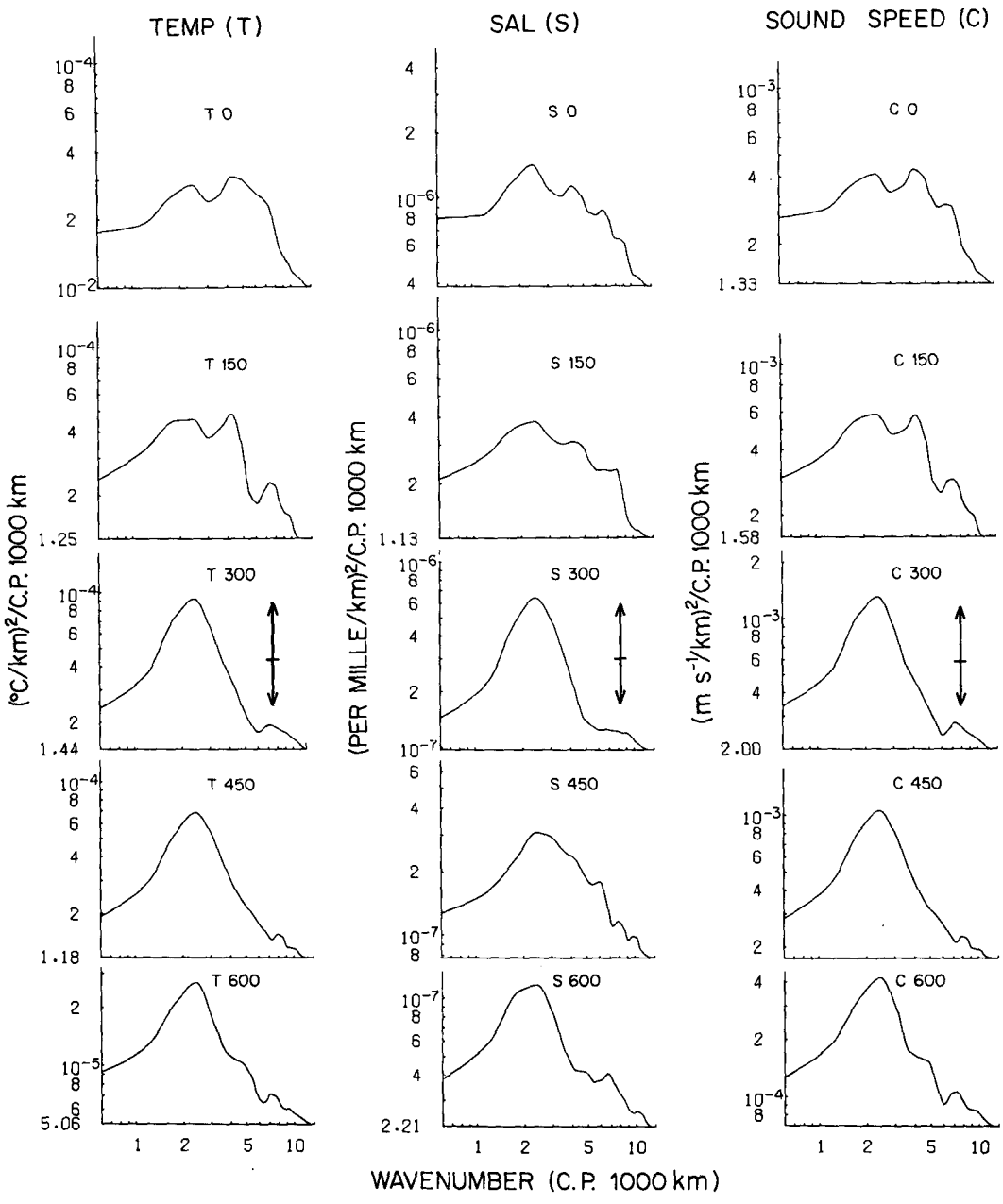

FIG. 4. Power density spectra of meridional gradients of temperature, salinity and sound velocity along longitude 168°E. Arrows indicate the 80% confidence limits.

few sections with a station spacing of 50 km or closer exist. The results given below are of a tentative nature, therefore.

The power density spectra for the zonal gradients of temperature, salinity, sound velocity and density at latitude 20°40′N are shown in Fig. 9 for the zonal wavenumber range between 0.6 and 13.4 c.p. 1000 km. The arrows indicate the 80% confidence limits. The spectra indicate two peaks: one at a wavenumber of about 1.5 c.p. 1000 km, corresponding to a wavelength of approximately 666 km, and the other at a wavenumber of 6.8 c.p. 1000 km, corresponding to a wavelength of about 150 km. Beyond 10 c.p. 1000 km, the spectral densities decrease rapidly with increasing zonal wavenumber.

In Fig. 10 (left) is shown the zonal wavenumber spectrum derived from Wilson and Dugan's (1978) observations. The spectrum represents the zonal gradient of the 12°C isotherm depth at latitudes 30°30′–32°N and is based on a multi-ship coordinated

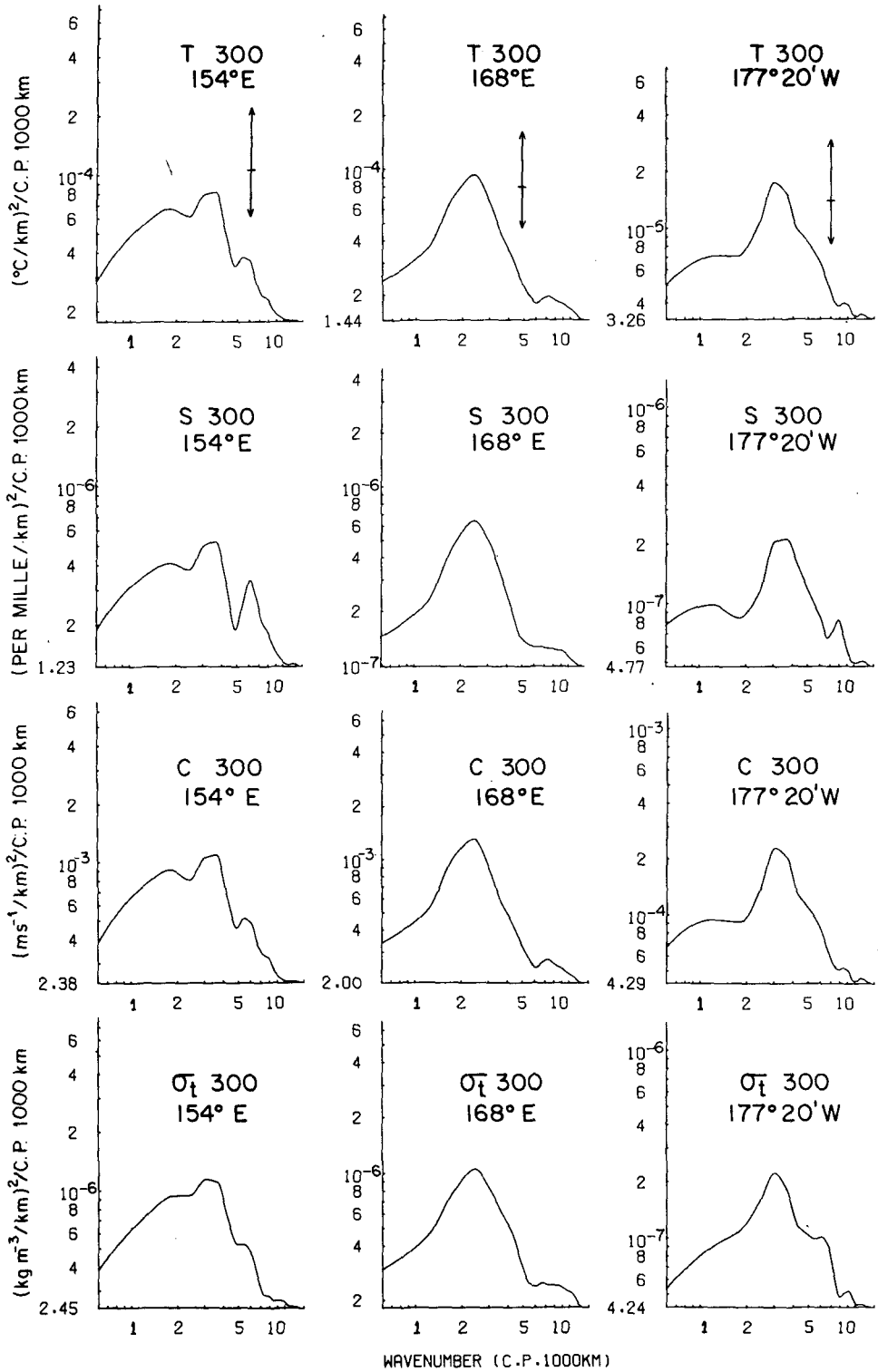

FIG. 5. Power density spectra of meridional gradients of temperature, salinity, sound velocity and density at 300 m, at longitudes 154°E, 168°E and 177°20'W. Arrows indicate the 80% confidence limits.

west-to-east expendable bathythermograph (XBT) survey. The spectrum shows a statistically significant peak at a wavenumber of 2 c.p. 1000 km. The wavenumbers corresponding to the half peak power are 1.8 and 3.5 c.p. 1000 km, respectively. This indicates that wavelengths between 285 and 555 km are common and that the most frequently encountered wavelength is 500 km. There is a sharp

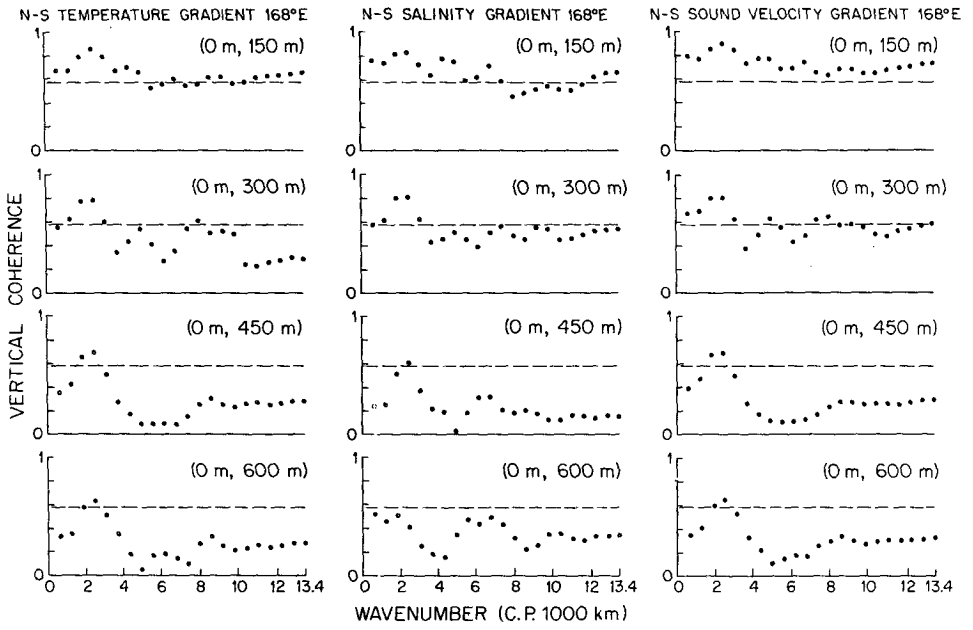

FIG. 6. Coherence between the meridional gradients at the sea surface and those at other depths along longitude 168°E. The dashed line indicates the 95% confidence limit.

decrease in power spectral density beyond 10 c.p. 1000 km, just as in the case discussed above.

In Fig. 10 (right) is shown the spectrum of the zonal temperature gradient at 300 m, derived from Bernstein and White's (1977) data. It is based on ship-of-opportunity XBT data between 35 and 38°N during the year 1975. The spectrum shows a statistically significant peak at 2 c.p. 1000 km, in agreement with Wilson and Dugan's (1978) findings. At wavenumbers beyond 4 c.p. 1000 km (dashed) the

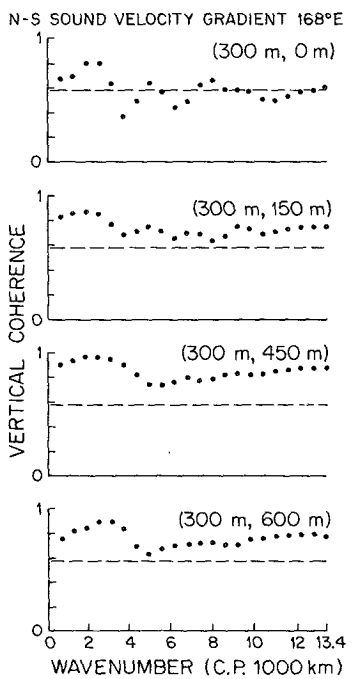

FIG. 7. Coherence between meridional sound velocity gradients at 300 m with those at other depths along longitude 168°E. The dashed line indicates the 95% confidence limit.

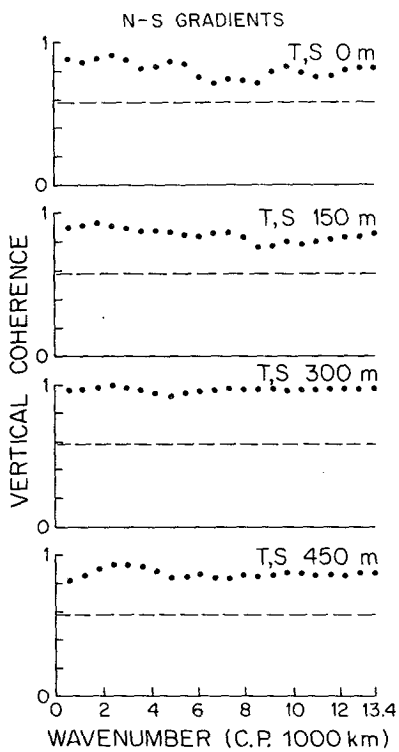

FIG. 8. Coherence between meridional gradients of temperature and salinity along lontitude 168°E. The dashed line indicates the 95% confidence limit.

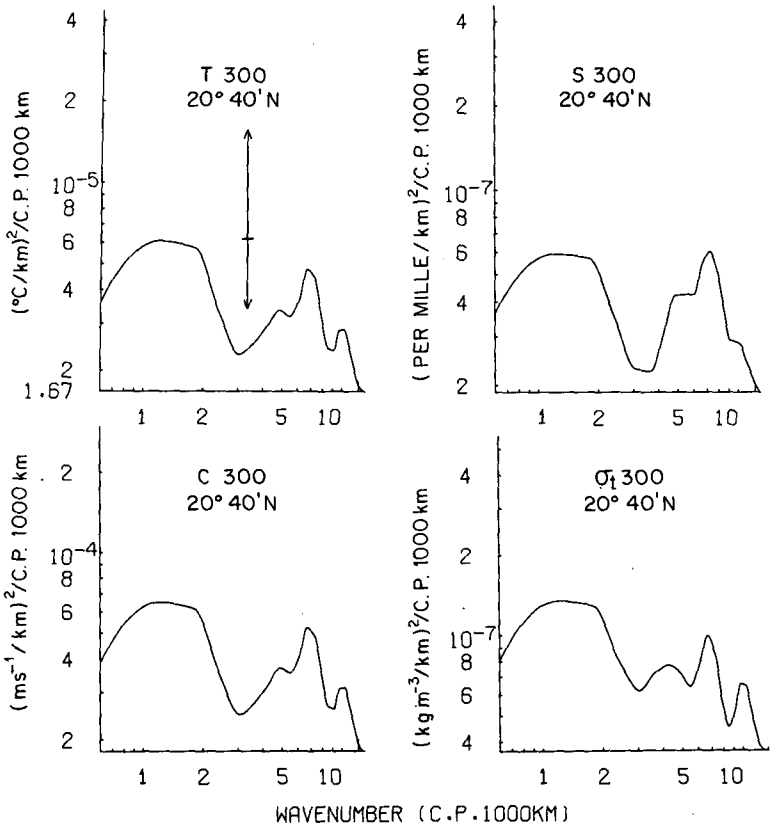

FIG. 9. Power density spectra of zonal gradients of temperature, salinity, sound velocity and density at 300 m, at latitude 20°40'N. The arrow indicates the 80% confidence limit.

power density does not decrease with increasing wavenumber. This behavior of the spectrum at high wavenumbers is atypical of the gradient spectra investigated so far and may result from instrumental limitations.

9. Oscillations of dynamic height in the western Pacific

The spectra of thermohaline and sound velocity gradients below pycnocline depth suggest the pres-

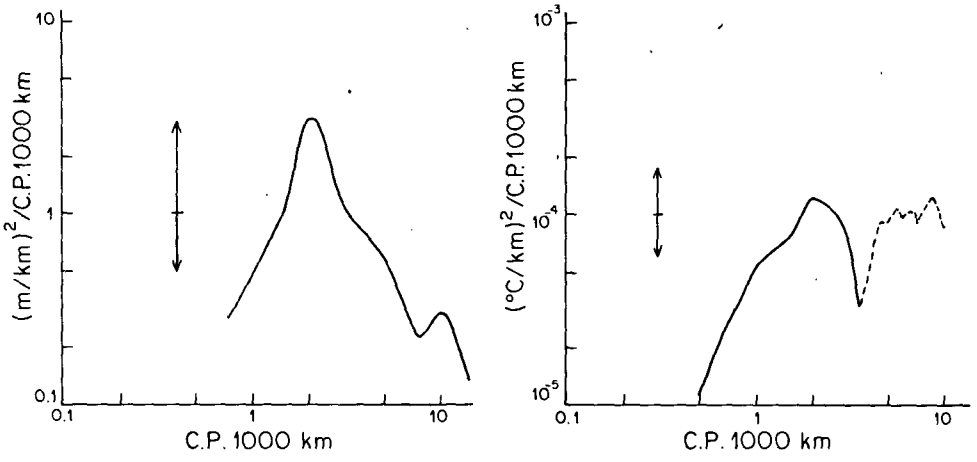

FIG. 10. Power density spectrum of the zonal gradient of the depth of the 12°C isotherm, based on Wilson and Dugan's (1978) data (left), and power density spectrum of the zonal temperature gradient at 300 m, based on Bernstein and White's (1977) data (right). The arrows indicate the 95% confidence limits.

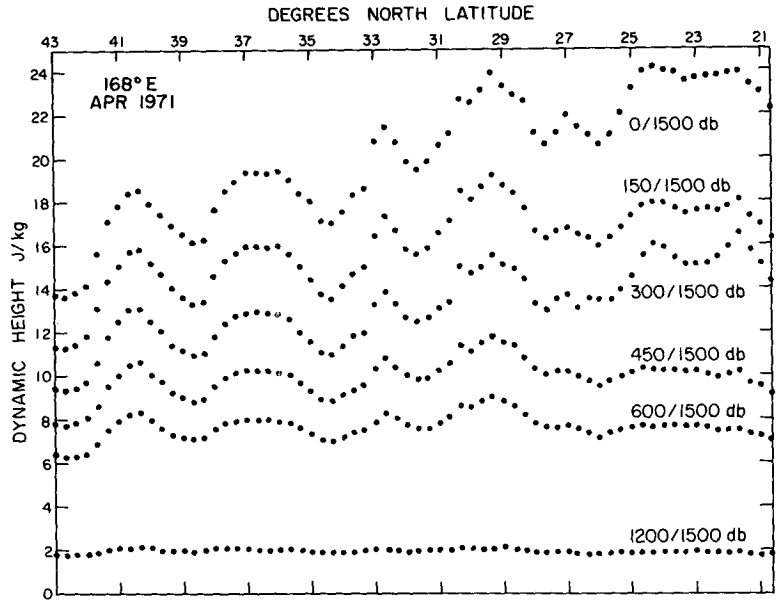

FIG. 11. Oscillations of dynamic heights, relative to 1500 db, along longitude 168°E in early April 1971.

ence of oscillations of 300–600 km wavelength. It is of interest to know whether similar oscillations occur in dynamic height.

In Fig. 11 are shown the dynamic heights relative to 1500 db along longitude 168°E. Oscillations of approximately 400 km length are prominent in the upper 600 m. Maximum amplitudes are close to 5 J kg^{-1}, equivalent to about 50 cm in sea surface elevation. The amplitudes appear to attenuate exponentially with depth: one-half the amplitude is encountered at 300 m and one-quarter at 600 m. Similar attenuation rates were observed in the central Pacific (Roden, 1977).

The power density spectrum for the 0/1500 db dynamic heights is shown in Fig. 12. A single prominent peak centered at 2.14 c.p. 1000 km stands out. The spectrum of the dynamic height gradient can be derived from the above by multiplying through by the wavenumber squared. When this is done, the peak shifts to 2.4 c.p. 1000 km, indicating a dominant wavelength of about 400 km. This is the same as found for the meridional thermohaline gradients below pycnocline depth.

8. Conclusions and discussion

The following conclusions can be drawn from an analysis of thermohaline and sound velocity gradients in the western North Pacific:

1) Strong meridional gradients, some of which attain frontal intensity (exceeding three times the rms gradient) are not limited to the surface layer, but occur at depths to 600 m. Many of the deep fronts have no surface manifestation, making detection from space difficult.

2) Fronts in the upper layer are spaced irregularly, while those between 300 and 600 m are spaced at quasi-regular intervals. This suggests that the dynamic processes of gradient formation differ for the upper and lower layers of the sea.

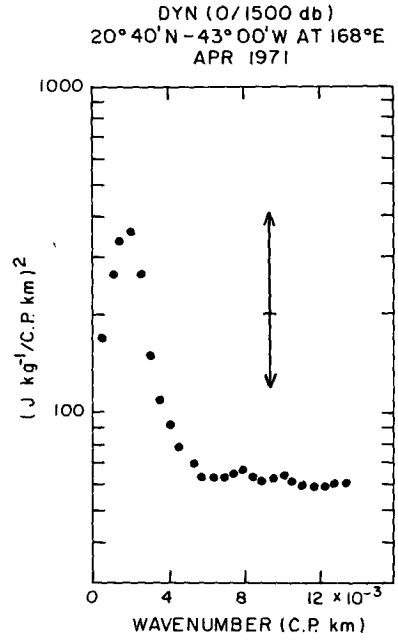

FIG. 12. Power density spectrum of the 0/1500 dynamic heights along longitude 168°E. The arrow indicates the 80% confidence limit.

3) The rms and extreme meridional gradients west of the Emperor seamount chain are considerably larger than to the east of it.

4) The shape of the power density spectra of meridional gradients depends strongly upon depth. In the upper 150 m, the shape is irregular. Between 300 and 600 m a well-defined peak is observed. The peak is broad and indicates that oscillations with a wavelength between 300 and 600 km are common. Beyond 10 c.p. 1000 km, the power density becomes very low, which suggests a cutoff wavelength of about 100 km.

5) The power density spectra of the meridional gradients show some dependence on longitude. The power levels west of the Emperor seamount chain are substantially higher than those to the east. Whether the differences in wavelengths associated with the spectral peaks (274 km at 154°E, 411 km at 168°E and 329 km at 177°20'W) are significant, cannot be determined from the limited data on hand.

6) Meridional gradients at the sea surface are coherent with those in the upper 150 m and incoherent with those below. Meridional gradients at 300 m have a good coherence with those at greater depths. This indicates that the surface and deep fronts are largely unrelated and must be detected by different means.

7) Meridional gradients of temperature and salinity are coherent in the wavenumber range between 0 and 13.4 c.p. 1000 km. The coherence is better at subsurface depths than at the sea surface. The less good coherence at the sea surface results from radiative heat transfer and precipitation processes which act largely independent of each other.

8) The power density spectra of the zonal temperature gradients at 300 m show a broad peak at wavenumbers between 1 and 3 c.p. 1000 km. The information at hand is insufficient to determine whether latitudinal differences exist. It is of interest to note that the zonal and meridional wavenumber ranges associated with the peaks in the zonal and meridional spectra are approximately the same. This indicates that in midlatitudes of the western Pacific the dominant east-west and north-south wavelengths are about equal.

Several unanswered questions remain. It is not known definitely whether the observed features are due to Rossby-type waves or eddies. The observed wavelengths (300–600 km, typically) and the cutoff wavelength of about 100 km are compatible with existing theories of Rossby waves (Longuet-Higgins, 1975; Lighthill, 1967; Philander, 1978); but do not rule out other processes, such as eddy formation by flow over complicated bottom topography. It is not known whether the spectra and coherences change with season, and whether the wavenumbers associated with the spectral peaks are the same during the stormy and calmer seasons. The change of the spectra and coherences with distance from major topographic features, such as the Emperor seamount chain, requires further study.

Answers to the above problems depend to a large degree on an effective sampling program. Some of the problems involved are discussed by Woods (1977). In the future, remote sensing by satellites holds promise. Frontal features above pycnocline depth can be detected by microwave and infrared techniques (Legeckis, 1975). Frontal features below pycnocline depth can be detected, in principle, by satellite radar altimetry, though the method has yet to be applied. This method will work at deep baroclinic fronts, across which there is a large sea surface slope. The slope can be detected from radar altimetry and a knowledge of the shape of the earth's geoid (Leitao *et al.*, 1978).

Acknowledgments. I am indebted to C. A. Barnes, L. H. Larsen and M. Rattray for advice. K. Bhatia carried out the programming. The scientific and operational crew of the R.V. *Thomas G. Thompson*, Captain Robert Schelling commanding, are to be commended for outstanding performance. The research reported herein was supported by the Office of Naval Research under Contract N-00014-75-C-0502, Project NR 083-012.

REFERENCES

Bernstein, R. L., and W. B. White, 1974: Time and length scales of baroclinic eddies in the central North Pacific Ocean. *J. Phys. Oceanogr.*, **4**, 613–624.

——, and ——, 1977: Zonal variability in the distribution of eddy energy in the mid-latitude North Pacific Ocean. *J. Phys. Oceanogr.*, **7**, 123–126.

Cheney, R. E., 1977: Synoptic observations of the oceanic frontal system of Japan. *J. Geophys. Res.*, **82**, 5459–5468.

Kawai, H., 1972: Hydrography of the Kuroship Extension. *Kuroshio: Physical Aspects of the Japan Current*, H. Stommel and K. Yoshida, Eds., University of Washington Press, 235–341.

Kirwan, A. D., 1975: Oceanic velocity gradients. *J. Phys. Oceanogr.*, **5**, 729–735.

Legeckis, R., 1975: Application of synchronous meterological satellite date to the study of time dependent sea surface temperature change along the boundary of the Gulf Stream. *Geophys. Res. Lett.*, **2**, 435–538.

Leitao, C. D., N. E. Huang, and C. G. Parra, 1978: Remote sensing of Gulf Stream using GEOS-3 radar altimeter. NASA Tech. Pap. 1209, 31 pp.

Lighthill, M. J., 1967: On waves generated in dispersive systems by travelling forcing effects, with application to the dynamics of rotating fluids. *J. Fluid Mech.*, **27**, 725–752.

Longuet-Higgins, M. S., 1965: The response of a stratified ocean to stationary or moving wind systems. *Deep-Sea Res.*, **12**, 923–973.

Palmén, E., and C. W. Newton, 1969: *Atmospheric Circulation Systems*. Academic Press, 602 pp.

Philander, S. G., 1978: Forced oceanic waves. *Rev. Geophys. Space Phys.*, **16**, 15–43.

Roden, G. I., 1972: Temperature and salinity fronts at the

boundaries of the subarctic-subtropical transition zone in the western Pacific. *J. Geophys. Res.*, **77**, 7175–7187.

——, 1975: On North Pacific temperature, salinity, sound velocity and density fronts, and their relation to the wind and energy flux fields. *J. Phys. Oceanogr.*, **5**, 557–571.

——, 1977: On long wave disturbances of dynamic height in the North Pacific. *J. Phys. Oceanogr.*, **7**, 41–49.

Shapiro, M. A., 1970: On the applicability of the geostrophic approximation to upper level frontal scale motions. *J. Atmos. Sci.*, **27**, 408–720.

Tolstoy, I., and C. S. Clay, 1966: *Ocean Acoustics*. McGraw-Hill, 293 pp.

Uda, M., 1938: Researches on "siome" or current rip in the seas and oceans. *Japan Geophys. Mag.*, **11**, 307–372.

Wilson, W. S., and J. P. Dugan, 1978: Mesoscale thermal variability in the vicinity of the Kuroshio Extension. *J. Phys. Oceanogr.*, **8**, 537–540.

Woods, J. D., 1977: Information theory related to experiments in the upper ocean. *Modelling and Prediction of the Upper Layers of the Ocean*, Pergamon Press, 263–283.